

The FERRUM project: transition probabilities for forbidden lines in [Fe II] and experimental metastable lifetimes

J. Gurell¹, H. Hartman², R. Blackwell-Whitehead², H. Nilsson², E. Bäckström¹, L. O. Norlin³, P. Royen¹, and S. Mannervik¹

¹ Department of Physics, Stockholm University, AlbaNova University Center, 10691 Stockholm, Sweden
e-mail: jonas.gurell@physto.se

² Lund Observatory, Lund University, Box 43, 22100 Lund, Sweden

³ Department of Physics, Royal Institute of Technology, AlbaNova University Center, 10691 Stockholm, Sweden

Received 3 September 2009 / Accepted 2 October 2009

ABSTRACT

Context. Accurate transition probabilities for forbidden lines are important diagnostic parameters for low-density astrophysical plasmas. In this paper we present experimental atomic data for forbidden [Fe II] transitions that are observed as strong features in astrophysical spectra.

Aims. We measure lifetimes for the $3d^6(^3G)4s\ a^4G_{11/2}$ and $3d^6(^3D)4s\ b^4D_{1/2}$ metastable levels in Fe II and experimental transition probabilities for the forbidden transitions $3d^7\ a^4F_{7/2,9/2}-3d^6(^3G)4s\ a^4G_{11/2}$.

Methods. The lifetimes were measured at the ion storage ring facility CRYRING using a laser probing technique. Astrophysical branching fractions were obtained from spectra of Eta Carinae, obtained with the Space Telescope Imaging Spectrograph onboard the *Hubble Space Telescope*. The lifetimes and branching fractions were combined to yield absolute transition probabilities.

Results. The lifetimes of the $a^4G_{11/2}$ and the $b^4D_{1/2}$ levels have been measured and have the following values, $\tau = 0.75 \pm 0.10$ s and $\tau = 0.54 \pm 0.03$ s respectively. Furthermore, we have determined the transition probabilities for two forbidden transitions of $a^4F_{7/2,9/2}-a^4G_{11/2}$ at 4243.97 and 4346.85 Å. Both the lifetimes and the transition probabilities are compared to calculated values in the literature.

Key words. atomic data – methods: laboratory – techniques: spectroscopic – stars: individual: Eta Carinae

1. Introduction

The cosmic abundance of iron is relatively high compared to other iron group elements and the spectrum of singly ionized iron, Fe II, is a significant contributor to the spectral opacity of the sun and hotter stars. The complex energy level structure of Fe II makes the spectrum extremely line rich and it has been studied in great detail with more than 1000 energy levels identified in the literature (Johansson 2009).

Fe II lines are observed in the spectra of a wide variety of astronomical objects, and there is a considerable demand for accurate atomic data for this ion. To meet the accurate data requirements of modern astrophysics, a program was initiated to supply the astronomical community with reliable atomic data: the FERRUM-project (Johansson et al. 2002). The aim of this international collaboration is to measure and evaluate astrophysically relevant experimental and theoretical transition data for the iron group elements.

There are 62 metastable levels in Fe II. The parity forbidden lines from some of these levels are observed as prominent features in astrophysical low density plasmas, such as nebulae, H II regions and circumstellar gas clouds. However, metastable levels have radiative lifetimes several orders of magnitude longer than other levels and are thus more affected by collisions. Due to the absence of these lines in laboratory spectra, the majority of forbidden line transition probabilities

(*A*-values) available in the literature are from theoretical calculations.

There are only four metastable levels in Fe II with laboratory measured lifetimes. The $a^6S_{5/2}$ and $b^4D_{7/2}$ levels have been measured by Rostohar et al. (2001) using laser probing of a stored ion beam (a laser probing technique, LPT). In addition, the $a^4G_{9/2}$ and $b^2H_{11/2}$ levels have been measured by Hartman et al. (2003) using the LPT. There is good agreement between Rostohar et al. (2001) and the calculated values of Nussbaumer et al. (1981) and Quinet et al. (1996). However, the lifetimes of Rostohar et al. (2001) are systematically shorter than the calculations of Garstang (1962). Hartman et al. (2003) also combined the lifetimes of $a^6S_{5/2}$, $b^4D_{7/2}$ and $a^4G_{9/2}$ with branching fractions (*BF*s) to determine experimental *A*-values for forbidden transitions. Hartman et al. (2003) measured the *BF*s in astrophysical spectra observed in the ejecta of Eta Carinae and presented additional theoretical *A*-value calculations.

We present radiative lifetimes for the $a^4G_{11/2}$ and $b^4D_{1/2}$ metastable levels in Fe II measured using the LPT at the CRYRING facility. In addition, *BF*s for two forbidden transitions 4243.97 Å and 4346.85 Å ($a^4F_{9/2}-a^4G_{11/2}$ and $a^4F_{7/2}-a^4G_{11/2}$) have been measured in astrophysical spectra observed in the ejecta of Eta Carinae recorded with the *Hubble Space Telescope* (*HST*) Space Telescope Imaging Spectrograph (STIS). The radiative lifetimes have been combined with the *BF*s to yield *A*-values and we provide a comparison with theoretical values in the literature.

2. Experimental measurements

The lifetime (τ) of a level i is defined as the inverse of the total transition probability (A_{ik}) for all possible decay channels from that level, according to Eq. (1), where k is summed over all lower levels.

$$\tau_i = \frac{1}{\sum_k A_{ik}}. \quad (1)$$

The majority of all excited levels will decay through electric dipole ($E1$) transitions which typically gives a lifetime of the order of a nanosecond, but if no allowed $E1$ decay channels are available, i.e. the level is metastable, the population decay has to be through higher order transitions associated with magnetic dipole or electric quadrupole terms. The probability for such a transition to occur is several orders of magnitude smaller compared to the probability for an $E1$ transition which makes the lifetime of a metastable level significantly longer, typically several milliseconds, seconds, minutes or even hours.

The BF of a transition ik is defined as the transition probability, A_{ik} , for a single line divided by the sum of the transition probabilities from all lines with the common upper level according to Eq. (2).

$$BF_{ik} = \frac{A_{ik}}{\sum_k A_{ik}}. \quad (2)$$

By combining Eqs. (1) and (2) the absolute transition probability, referred to as the A -value, of each decay channel can be deduced according to Eq. (3).

$$A_{ik} = \frac{BF_{ik}}{\tau_i}. \quad (3)$$

2.1. Lifetime measurements of metastable Fe II levels

The lifetimes of the two metastable levels were measured using the LPT (Lidberg et al. 1999; Mannervik 2003; Mannervik et al. 2005) at the ion storage ring CRYRING at the Manne Siegbahn laboratory in Stockholm, Sweden. The LPT has been developed and refined during several years and has been used to measure lifetimes ranging from 3.4 ms in Xe II (Lidberg et al. 1997) to 89 s in Ba II (Gurell et al. 2007).

A hot ion source is used to produce ions that can be extracted and injected into the storage ring. Once inside CRYRING, singly charged ions may be stored for several minutes at 40 keV and investigated in this ultra high vacuum environment with a background pressure lower than 10^{-11} Torr. For the experiment described in this paper Fe⁺ ions were produced in a Nielsen ion source used in combination with an oven filled with FeCl₂. By heating the oven to approximately 400 °C and running the ion source with argon as a carrier gas it was possible to extract and store a current of Fe⁺ ions as high as 4 μ A in CRYRING.

Ions in excited states will decay as they are being stored and by passively monitoring the excited level population, a decay curve can be constructed. However, the low intensity of forbidden transitions is hard to detect directly since the emission is spread out over the 52 m length of the storage ring and spread across the 4π solid angle. A LPT in combination with a Doppler tuning device (DTD) was used to increase the strength of the signal. The LPT probes the population of the metastable level by laser-inducing a transition to a higher lying short lived level. Within a few ns this level will decay to another lower lying level and the fluorescence originating from that transition is used as an indirect measurement of the population of the metastable level at

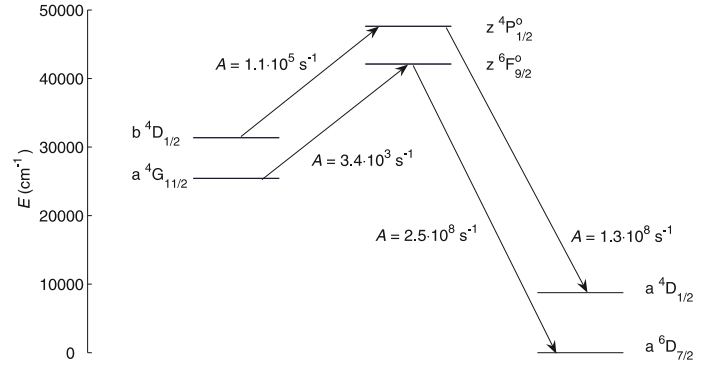


Fig. 1. Probing scheme for the two levels studied. The populations of the metastable levels, shown in the left side of the figure, were probed through excitation to the higher lying levels in the middle of figure. Once in the higher lying excited levels the populations decay to lower lying levels, shown in the right side of the figure. The intensity of this fluorescence is detected and used as a relative measurement of the original population of the metastable level under study. See the text for references to the cited A -values.

the time of the probe pulse's arrival. The probing scheme used in this study is shown in Fig. 1 with A -values from Baschek et al. (1970), Kostyk & Orlova (1982) and Ralchenko et al. (2008) and energy levels from Johansson (1978).

The DTD was used to locally accelerate the ions in front of our detector, thereby inducing a Doppler shift. A narrow band ring dye laser was used to tune the resonance of the ions within the small volume of a few cm³ that constitutes the DTD. This technique forces the probing as well as the following rapid fluorescence to occur in front of the detector which greatly enhances the photon count.

We used a Coherent 699-29 ring dye laser, operated with a Rhodamine 6G dye and pumped by a Coherent Innova 400-25 argon laser, to produce laser light with the desired wavelengths of 5985 and 6143 Å. The fluorescence was monitored with a Hamamatsu R585 photomultiplier tube in front of which an optical filter was mounted in order to reduce the background signal coming from scattered laser light.

The populations of the metastable levels under study were probed as a function of delay time after ion injection. Every fourth ion injection was used to measure the laser induced fluorescence at a fixed time after injection in order to make sure that the initial population of the level of interest did not change during the data acquisition time.

2.1.1. Collisional quenching

The small amount of residual gas in the storage ring gives rise to collisional quenching of the metastable levels. Therefore, it is necessary to measure the decay rate of the level population as a function of pressure and extrapolate to zero pressure in order to get the pure radiative decay rate. The decay rate has a linear dependence and the extrapolation can be determined with a Stern-Vollmer plot (Demtröder 1996). In practice this is achieved by allowing the residual gas pressure inside CRYRING to be varied by heating a non-evaporative getter pump, which releases previously absorbed rest gas thereby increasing the pressure slightly. The operating pressure inside CRYRING is out of the range of standard vacuum meters and a relative pressure measurement has to be used instead. Once stored, ions are gradually neutralized

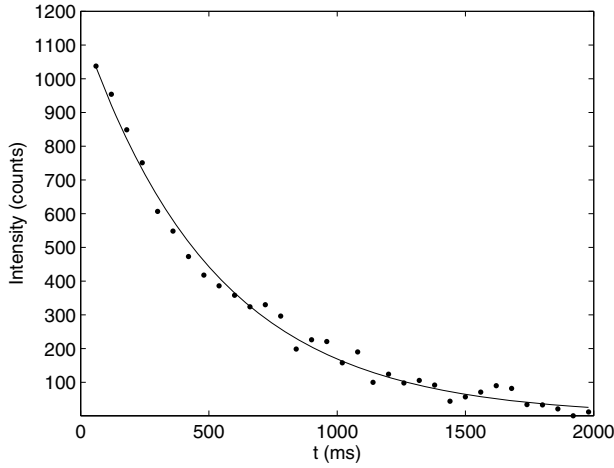


Fig. 2. Observed population decay curve of the $3d^6(^3D)4s b^4D_{1/2}$ level.

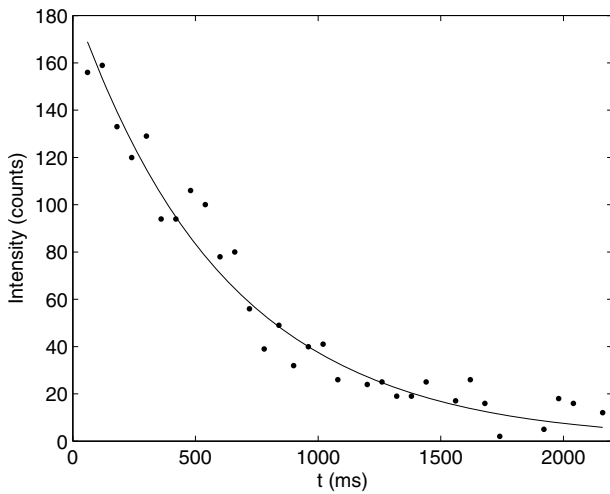


Fig. 3. Observed population decay curve of the $3d^6(^3G)4s a^4G_{11/2}$ level.

due to collisions with the rest gas and the number of ions stored undergoes an exponential decay as a function of time after injection. This decay rate of the ion beam is assumed to be inversely proportional to the rest gas pressure and is used as a relative pressure measurement. The decay of the ion beam is measured with a multi-channel plate connected to the CRYRING storage ring.

The extrapolations of the decay rates to zero pressure were made in two Stern-Vollmer plots shown in Figs. 4 and 5. The data were fitted with a linear fit weighted against the inverse uncertainty in each data point. The uncertainty of the extrapolated pure radiative decay rate is given as the standard deviation of the fit in the corresponding Stern-Vollmer plot.

2.1.2. Repopulation

Collisional excitation of ground state ions into metastable levels, referred to as repopulation, is usually corrected for when using the LPT for lifetime measurements, see e.g. Royen et al. (2007). An attempt to measure the repopulation in this study was made but the signal was below the background level of approximately 5 photons per second which makes the collisional excitation effect negligible. The production of metastable ions at the time of ion injection was monitored and showed stable conditions throughout the experiment. Decay curves for the populations of the two levels are shown in Figs. 2 and 3 together with the fitted

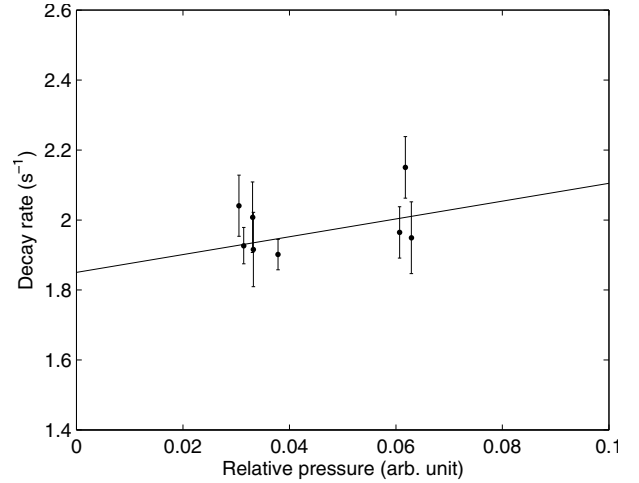


Fig. 4. Stern-Vollmer plot showing the decay rate of the $3d^6(^3D)4s b^4D_{1/2}$ level population as a function of pressure.

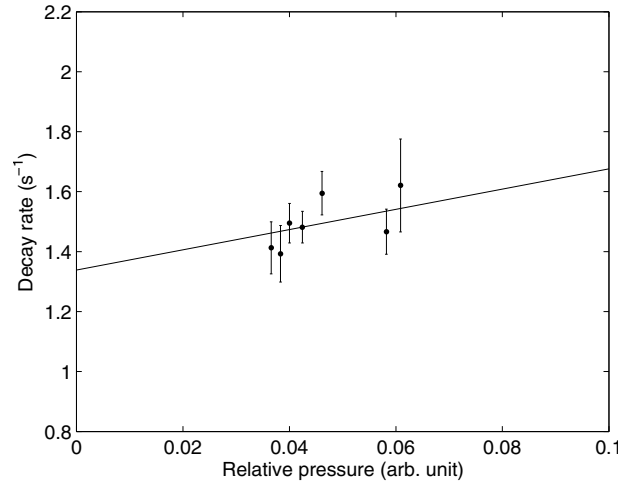


Fig. 5. Stern-Vollmer plot showing the decay rate of the $3d^6(^3G)4s a^4G_{11/2}$ level population as a function of pressure.

curves used to determine the lifetimes of the levels. The standard deviation of each fit was used as the uncertainty in the particular lifetime curve.

2.2. Astrophysical branching fractions for $a^4G_{11/2}$

The intensity of an emission line is proportional to the product NA where N is the population of the upper level and A is the transition rate of the transition. For lines having the same upper level the observed photon intensity is proportional to the transition rate. Together with Eq. (2) this relates the BF to the measured intensities for all the decay channels from a single upper level:

$$BF_{ik} = \frac{A_{ik}}{\sum_k A_{ik}} = \frac{I_{ik}}{\sum_k I_{ik}}. \quad (4)$$

For electric dipole transitions, the branching fractions are often determined using a standard laboratory light source with a high-density plasma and high resolution spectrometer. However, the A -value of a forbidden line is typically 10^6 – 10^9 times lower than the A -value of an allowed transition which makes the forbidden lines too weak to be observed in the spectrum of a standard laboratory source. To observe strong forbidden lines the ions must

Table 1. Experimentally determined lifetimes of metastable levels in Fe II. The uncertainties are given in brackets.

Configuration	Term	This work	Ref. [1]	Ref. [2]	τ (s)				
					Ref. [3]	Ref. [4]	Ref. [5]	Ref. [6]	Ref. [7]
$3d^5 4s^2$	$a^6S_{5/2}$		0.23(3)		0.326	0.235	0.262	0.220	0.222
$3d^6(^3G)4s$	$a^4G_{11/2}$	0.75(10)			0.852		0.774	0.704	
$3d^6(^3G)4s$	$a^4G_{9/2}$			0.65(2)	0.856		0.755	0.694	
$3d^6(^3H)4s$	$b^2H_{11/2}$			3.8(3)	10.1		6.59	5.20	
$3d^6(^3D)4s$	$b^4D_{1/2}$	0.54(3)			0.677		0.630	0.550	
$3d^6(^3D)4s$	$b^4D_{7/2}$		0.53(3)		0.618		0.567	0.500	
References:	[1] Rostohar et al. (2001) (Experimental) [2] Hartman et al. (2003) (Experimental) [3] Garstang (1962) (Calculated) [4] Nussbaumer et al. (1981) (Calculated, Superstructure code) [5] Quinet et al. (1996) (Calculated, Superstructure) [6] Quinet et al. (1996) (Calculated, relativistic Hartree-Fock) [7] Hartman et al. (2003) (Calculated, CIV3 code)								

be kept in a low-density plasma environment, to minimize the collisional deexcitation (quenching), and in a large volume, to get a critical number of ions. Low density astrophysical plasmas fulfil these criteria, and their spectra often show strong forbidden lines. In particular, the spectra of the Weigelt blobs in Eta Carinae are rich in forbidden transition from the iron group including the [Fe II] 4243 and 4346 Å lines and Weigelt blob spectra observed by HST STIS have been used in this study. A great advantage of using HST STIS is the high angular resolution ($0''.1$) which minimizes the contribution from surrounding regions. In addition, the spectrum of the Weigelt blobs has been studied in great detail (e.g. Zethson 2001), which decreases the uncertainty from blending lines or misinterpretations of spectral features.

Astrophysical BF s have similar uncertainties to laboratory measurements including uncertainties in the intensity measurements, intensity calibration and unobservable lines (Sikström et al. 2002). Additional uncertainties include corrections for interstellar reddening and blending from other spatial regions along the line of sight. Furthermore, a standard reddening curve was used to correct for reddening. However, the reddening effect was found to be only a few percent because the lines are separated by a relative narrow wavelength range of 100 Å. The uncertainties have been treated in accordance with the guidelines the National Institute of Standards and Technology, USA (Taylor & Kuyatt 1994).

3. Results

A summary of the lifetime measurements and a comparison to theoretical values in the literature is given in Table 1. For the $3d^6(^3G)4s a^4G_{11/2}$ level $\tau = 0.75 \pm 0.10$ s and for the $3d^6(^3D)4s b^4D_{1/2}$ level $\tau = 0.54 \pm 0.03$ s. Theoretical calculations indicate that unobserved branching transitions for the $a^4G_{11/2}$ level constitute less than 4% of the total BF (Quinet et al. 1996). The large relative uncertainty associated with the $a^4G_{11/2}$ lifetime is due to a lower number of photon counts per second compared to the detection of fluorescence following excitation from the $b^4D_{1/2}$ level. This is mainly due to the difference in the A -values of the two probing transitions used, see Fig. 1, which differ by almost two orders of magnitude. The experimental conditions not associated with the internal structure of the atomic system (i.e. laser power, background pressure, ion current, optical alignment etc.) remained very similar during the two lifetime measurements.

Table 2. Experimentally determined transition probabilities compared to theoretical values from a $^4G_{11/2}$.

Transition	λ_{air} (Å)	A (s^{-1})		
		This work	Quinet et al. (1996) SST	HFR
$a^4F_{9/2} - a^4G_{11/2}$	4243.97	1.05(15)	1.02	1.12
$a^4F_{7/2} - a^4G_{11/2}$	4346.85	0.25(5)	0.23	0.25

We have measured astrophysical BF s for lines from a $^4G_{11/2}$, from which the strongest decay channels are to 4F at 4243 and 4346 Å. The transitions from $b^4D_{1/2}$ are distributed over a larger wavelength region than transitions from a $^4G_{11/2}$, and many of the lines are blended with other lines making the intensity measurements uncertain. Therefore we could not derive BF s for lines from this level. The experimental A -values are given in Table 2, along with uncertainties and comparisons to calculations. The agreement with the values by Quinet et al. (1996) is within our uncertainties. We estimate the uncertainty of the BF s to 6–12%, including the uncertainties in the intensity measurement, calibration, reddening and residual lines.

4. Discussion

The relativistic Hartree-Fock (HFR) calculations by Quinet et al. (1996) show the best general agreement with the experimental values presented in this and previous studies. The agreement is good with the exception of the $b^2H_{11/2}$ level (Rostohar et al. 2001) which differs by 5σ . This deviation has been explained by Hartman et al. 2003 as an effect of level mixing between the $b^2H_{11/2}$ and the $a^4G_{11/2}$ levels. In addition, this mixing has been observed by Johansson (1978) through unexpected spin forbidden spectral lines, e.g. the $b^2H_{11/2} - z^6F_{9/2}$ transition at 6269.97 Å.

Comparison of the theoretical lifetime values in Table 1 for a $^4G_{11/2}$ and $b^2H_{11/2}$ indicate that the lifetime of the $a^4G_{11/2}$ level should be approximately one tenth of the lifetime of $b^2H_{11/2}$. However, the experimental values reveal that the $a^4G_{11/2}$ level is only one fifth of the lifetime for $b^2H_{11/2}$ indicating that the mixing effect can be observed in the lifetimes. Calculations are sensitive to level mixing and performing ab initio calculations which reproduce the mixing properties

of the system is not trivial. This is illustrated in Nahar & Pradhan (1994), Nahar (1995), Hibbert & Corrége (2005), Corrége & Hibbert (2006) and Pickering et al. (2002). In particular, Pickering et al. (2002) emphasized that even though the agreement between the theoretical and experimental Fe II A -values investigated by Pickering et al. (2002) are in general extremely good, probabilities related to spin forbidden transitions that occur due to level mixing may differ by up to an order of magnitude.

Acknowledgements. The authors acknowledge the help from the CRYRING staff. This work was supported by the Swedish Research Council (VR), the Swedish National Space Board (SNSB) and through a Linnaeus grant from VR. R.B.W. would like to acknowledge the European Commission for a Marie Curie Intra-European fellowship. This research has made use of the data archive for the HST Treasury Program on Eta Carinae (GO 9973) which is available online at <http://etacar.umn.edu>. The archive is supported by the University of Minnesota and the Space Telescope Science Institute under contract with NASA. In addition, we gratefully acknowledge the discussion with Prof. Selvelli on forbidden iron lines in RR Tel.

References

- Baschek, B., Garz, T., Holweger, H., & Richter J. 1970, A&A, 4, 229
 Corrége, G., & Hibbert, A. 2006, ApJ, 636, 1166
 Demtröder, W. 1996, Laser spectroscopy, Basic concepts and instrumentation, 2nd ed. (New York, Berlin: Springer)
 Garstang, R. H. 1962, MNRAS, 124, 321
 Gurell, J., et al. 2007, Phys. Rev. A, 75, 052506
 Hartman, H., Derkach, A., Donnelly, M. P., et al. 2003, A&A, 397, 1143
 Hibbert, A., & Corrége, G. 2005, Phys. Scr., T119, 61
 Johansson, S. 1978, Phys. Scr., 18, 217
 Johansson, S. 2009, Phys. Scr., T143, 014013
 Johansson, S., Derkach, A., Donnelly, M. P., et al. 2002, Phys. Scr., T100, 71
 Kostyk, R. I., & Orlova, T. V. 1982, Astrometiya Astrofiz., 47, 32
 Lidberg, J., Al-Khalili, A., Cowan, R. D., et al. 1997, Phys. Rev. A, 56, 4
 Lidberg, J., Al-Khalili, A., Norlin, L. O., et al. 1999, Nucl. Instrum. Methods Phys. Res. B, 152, 157
 Mannervik, S. 2003, Phys. Scr., T119, 49
 Mannervik, S., Ellmann, A., Lundin, P., et al. 2005, Phys. Scr., T105, 67
 Nahar, S. N. 1995, A&A, 293, 967
 Nahar, S. N., & Pradhan, A. K. 1994, J. Phys. B, 27, 429
 Nussbaumer, H., Pettini, M., & Storey, P. J. 1981, A&A, 102, 351
 Pickering, J. C., Donnelly, M. P., Nilsson, H., Hibbert, A., & Johansson, S. 2002, A&A, 396, 715
 Quinet, P., Le Dourneuf, M., & Zeippen, C. J. 1996, A&AS, 120, 361
 Ralchenko, Yu., Kramida, A. E., Reader, J., & NIST ASD Team (2008) NIST Atomic Spectra Database, version 3.1.5, <http://physics.nist.gov/asd3>; National Institute of Standards and Technology, Gaithersburg, MD
 Rostohar, D., Derkach, A., Hartman, H., Johansson, S., Lundberg, H., et al. 2001, Phys. Rev. Lett., 86, 8
 Royen, P., Gurell, J., Lundin, P., Norlin, L. O., & Mannervik, S. 2007, Phys. Rev. A, 76, 030502(R)
 Sikström, C. M., Nilsson, H., Litzen, U., Blom, A., & Lundberg, H. 2002, J. Quant. Spec. Rad. Trans., 74, 355
 Taylor, B. N., & Kuyatt, C. E. 1994, NIST Technical Note 1297, Guidelines for evaluating and expressing the uncertainty of NIST measurement results, National Institute of Standards and Technology, USA, <http://physics.nist.gov/Pubs/guidelines/>
 Zethson, T. 2001, Ph.D. Thesis, Lund University